The Astronomical Journal, 125:2341–2347, 2003 May

THE COMPACT NUCLEUS OF THE DEEP SILICATE ABSORPTION GALAXY NGC 4418[1]

A. S. Evans,[2] E. E. Becklin,[3] N. Z. Scoville,[4] G. Neugebauer,[5] B. T. Soifer,[5] K. Matthews,[5] M. Ressler,[6] M. Werner,[6] and M. Rieke[7]

Received 2002 October 30; accepted 2003 January 28

ABSTRACT

High-resolution *Hubble Space Telescope* (*HST*) near-infrared and Keck mid-infrared images of the heavily extinguished infrared-luminous galaxy NGC 4418 are presented. These data make it possible to observe the imbedded near-infrared structure on scales of 10–20 pc and to constrain the size of the mid-infrared–emitting region. The 1.1–2.2 μm data of NGC 4418 show no clear evidence of nuclear star clusters or of a reddened active galactic nucleus. Instead, the nucleus of the galaxy consists of a $\sim$100–200 pc linear structure with fainter structures extending radially outward. The near-infrared colors of the linear feature are consistent with a 10–300 Myr starburst suffering moderate levels (a few magnitudes) of visual extinction. At 7.9–24.5 μm NGC 4418 has estimated size upper limits in the range of 30–80 pc. These dimensions are consistent with the highest-resolution radio observations obtained to date of NGC 4418, as well as the size of 50–70 pc expected for a blackbody with a temperature derived from the 25, 60, and 100 μm flux densities of the galaxy. Further, a spectral energy distribution constructed from the multiwavelength mid-infrared observations shows the strong silicate absorption feature at 10 μm, consistent with previous mid-infrared observations of NGC 4418. An infrared surface brightness of $\sim 2.1 \times 10^{13}\ L_{\odot}$ kpc^{-2} is derived for NGC 4418. Such a value, though consistent with the surface brightness of warm ultraluminous infrared galaxies [$L_{\rm IR}(8\text{–}1000\ \mu{\rm m}) \geq 10^{12}\ L_{\odot}$], such as IRAS 05189−2524 and IRAS 08572+3915, is not large enough to distinguish NGC 4418 as a galaxy powered by an active galactic nucleus, as opposed to a lower surface brightness starburst.

Key words: galaxies: active — galaxies: individual (NGC 4418)

1. INTRODUCTION

Mid-infrared spectra of some infrared-luminous galaxies show a deep 10 μm silicate grain absorption feature believed to be a strong indication of a buried, compact energy source (Roche et al. 1986; Smith, Aiken, & Roche 1989; Dudley & Wynn-Williams 1997; Spoon et al. 2001). The nearest of these, the $L_{\rm IR}(8\text{–}1000\ \mu{\rm m}) \sim 8 \times 10^{10}\ L_{\odot}$ galaxy NGC 4418 (Roche et al. 1986), is a nearly edge-on Sa-type galaxy, which is likely interacting with a distorted companion galaxy 24 kpc away (see the Digitized Sky Survey image of the galaxy pair). NGC 4418 has a high infrared luminosity–to–molecular gas mass ratio [$L_{\rm IR}/M({\rm H_2}) \gtrsim 100$; Sanders, Scoville, & Soifer 1991][8] and warm infrared colors ($f_{25\mu{\rm m}}/f_{60\mu{\rm m}} = 0.23$) similar to those observed in infrared galaxies with Seyfert-like emission-line spectra; the latter property has led to speculation that the dust in NGC 4418 is being heated by an imbedded AGN. The optical spectrum of the galaxy has very faint Hα emission, but the forbidden lines of [N II] $\lambda\lambda$6548, 6583, [O I] λ6300, and [S II] $\lambda\lambda$6716, 6731 have not been detected, making it difficult to classify the galaxy as a Seyfert, LINER, or H II region–like galaxy (Armus, Heckman, & Miley 1989). No emission lines are detected at mid-infrared wavelengths (Spoon et al. 2001). The calculated visual extinction of greater than 50 mag derived from the observed silicate absorption feature verifies that optical observations reveal little about the nuclear regions.

As part of the larger program to image *IRAS*-luminous galaxies with the *Hubble Space Telescope* (*HST*) Near Infrared Camera and Multi-Object Spectrometer (NICMOS) and the Keck II Telescope with the mid-infrared camera MIRLIN, observations of NGC 4418 have been obtained. Both instruments are ideally suited for observations of infrared galaxies: NICMOS combines near-infrared technology with the excellent resolution possible with *HST* (0.″11 at 1.1 μm), making it possible to peer deeper into the optically obscured nuclear regions of infrared galaxies. MIRLIN combines mid-infrared technology with the large collecting area and the spatial resolution capabilities of the Keck telescope. These observations yield important insight into the environment of the central energy source of NGC 4418 and possibly into the nature of more distant and infrared-luminous galaxies with deep silicate absorption features. The NICMOS portion of this data set has been briefly discussed elsewhere (Scoville et al. 2000). Throughout this paper a distance to NGC 4418 of 27.3 Mpc (e.g., Ridgway, Wynn-Williams, & Becklin 1994) is adopted, such that 1″ subtends 130 pc at the distance of NGC 4418.

[1] Some of the data presented herein were obtained at the W. M. Keck Observatory, which is operated as a scientific partnership among the California Institute of Technology, the University of California, and the National Aeronautics and Space Administration. The Observatory was made possible by the generous financial support of the W. M. Keck Foundation.

[2] Department of Physics and Astronomy, Stony Brook University, Stony Brook, NY 11794-3800; aevans@mail.astro.sunysb.edu.

[3] Department of Physics and Astronomy, UCLA, Los Angeles, CA 90095.

[4] Division of Physics, Math, and Astronomy, Mail Stop 105-24, California Institute of Technology, Pasadena, CA 91125.

[5] Palomar Observatory, Mail Stop 320-47, California Institute of Technology, Pasadena, CA 91125.

[6] Jet Propulsion Laboratory, Mail Stop 169-506, 4800 Oak Grove Drive, Pasadena, CA 91109.

[7] Steward Observatory, University of Arizona, Tucson, AZ 85721.

[8] For spiral galaxies and for extreme star-forming giant molecular cloud cores, where stars are the main source of dust heating, $L_{\rm IR}/M({\rm H_2}) = 5$ and 25, respectively; Sanders & Mirabel (1996).

2. OBSERVATIONS AND DATA REDUCTION

2.1. *Near-Infrared Data*

HST observations of NGC 4418 were obtained on 1997 November 27 using the NICMOS2. NICMOS consists of three 256 × 256 HgCdTe arrays, each with a different pixel scale; the pixel scale of NICMOS2 is $0\farcs0762 \times 0\farcs0755$ pixel^{-1} in the x and y direction, providing a $19\farcs5 \times 19\farcs3$ field of view (Thompson et al. 1998). Images were obtained using the F110W (1.1 μm), F160W (1.6 μm), and F222M (2.2 μm) filters, providing resolutions of $0\farcs11$, $0\farcs16$, and $0\farcs22$, respectively. Observations were done by executing a four-point spiral dither per filter setting. At each dither position, nondestructive reads (MULTIACCUM) were obtained, with integration times of 88 s (1.1, 1.6 μm) and 120 s (2.2 μm) per exposure. In addition to the galaxy observations three-point spiral dither observations of 120 s each were done on blank sky (4′ south of NGC 4418) using the 2.2 μm filter. Finally, dark exposures were taken using the same MULTIACCUM sequences executed for the galaxy and sky observations.

Reduction of the data was done with IRAF.[9] The dark was first created, then the NICMOS data were dark-subtracted, flat-fielded, and corrected for cosmic rays using the IRAF pipeline reduction routine CALNICA (Bushouse 1997). The dithered images were then shifted and averaged using the DRIZZLE routine in IRAF (e.g., Hook & Fruchter 1997). The blank sky data were reduced in the same manner, and the measured 2.22 μm sky level of 0.45 ADU s^{-1} was subtracted from the 2.2 μm image of NGC 4418. Additional sky subtraction was performed for each band by removing an offset equal to the average pixel value near the edges of each image. Flux calibrations of the images were calculated using the conversion factors 2.031×10^{-6}, 2.190×10^{-6}, and 5.487×10^{-6} Jy (ADU s^{-1})$^{-1}$ at 1.1, 1.6, and 2.22 μm, respectively, and corresponding magnitude zero points of 1775, 1083, and 668 Jy.

To enhance the details seen in all three bands and to achieve a common resolution, all three images were deconvolved using the IRAF routine LUCY and a point-spread function (PSF) star observed on 1997 November 20 with the same filters and dither pattern as the NGC 4418 observations. The 1.1 and 1.6 μm images were then convolved with a Gaussian using the routine GAUSS, such that their resolutions matched that of the deconvolved 2.2 μm image ($\sim 0\farcs14$).[10] The resultant images are shown in Figures 1–2; Figure 1 shows the 1.1, 1.6, 2.2, and 1.6 μm/1.1 μm images separately in gray scale, and Figure 2 is a three-color image of NGC 4418.

2.2. *Mid-Infrared Data*

The mid-infrared observations of NGC 4418 were made on 1998 March 19 using the MIRLIN mid-infrared camera (Ressler et al. 1994) at the f/40 bent Cassegrain visitor port of the Keck II telescope. The camera uses a 128 × 128 Si : As array with a plate scale of $0\farcs138$ pixel^{-1}, for a total field of view of $17'' \times 17''$. Table 1 gives the central wavelengths and filter bandwidths for the filters through which the object was observed. At each wavelength the observing procedure was the same. A secondary mirror with a square wave chop of amplitude 6″ in the east-west direction at 4 Hz was employed for fast beam switching. The frames sampling each chop position were co-added separately in hardware, resulting in two images. After an interval of approximately a minute, the telescope was nodded perpendicular to the chop direction by 6″, and a second pair of images was obtained in order to cancel residuals in the sky and to subtract telescope emission. This procedure was repeated a number of times at each wavelength. The data were reduced by differencing the two images obtained within the chop pairs at each nod location and then co-adding the resulting positive images, with the positions appropriately adjusted to a common location, to yield a positive image centered in a field approximately $6'' \times 6''$. Because of the chopper and telescope nod spacings employed for the observations, the data are not capable of measuring flux outside a 6″ diameter region.

[9] IRAF is distributed by the National Optical Astronomy Observatory, which is operated by the Association of Universities for Research in Astronomy, Inc., under cooperative agreement with the National Science Foundation.

[10] This was achieved by first performing the same analysis on infrared galaxy images containing unresolved star clusters (see Scoville et al. 2000); the quoted resolution is the resolution of these star clusters after the analysis. Gaussians with different dispersions were applied to these images until one with the appropriate resolution was achieved.

TABLE 1
MID-INFRARED PHOTOMETRY

Name	Central Wavelength (μm)	Width (μm)	HR 1457 Magnitude[a] (mag)	NGC 4418 Magnitude[b] (mag)	NGC 4418 Flux Density[b,c] (mJy)
7.9	7.91	0.76	−2.99	4.85 ± 0.07	704
8.8	8.81	0.87	−3.01	5.62 ± 0.04	291
9.7	9.69	0.93	−3.03	5.98 ± 0.12	169
10.3	10.27	1.01	−3.04	6.60 ± 0.10	86
11.7	11.70	1.11	−3.06	5.27 ± 0.07	231
12.5	12.49	1.16	−3.07	3.51 ± 0.02	1030
17.9	17.90	2.00	−3.05	2.10 ± 0.04	1810
24.5	24.48	0.76	−3.03	−0.18 ± 0.03	7670

[a] Adopted.
[b] Using a 4″ diameter beam.
[c] The value of f_ν based on *IRAS* formulation for 0.0 mag (Beichman et al. 1989).

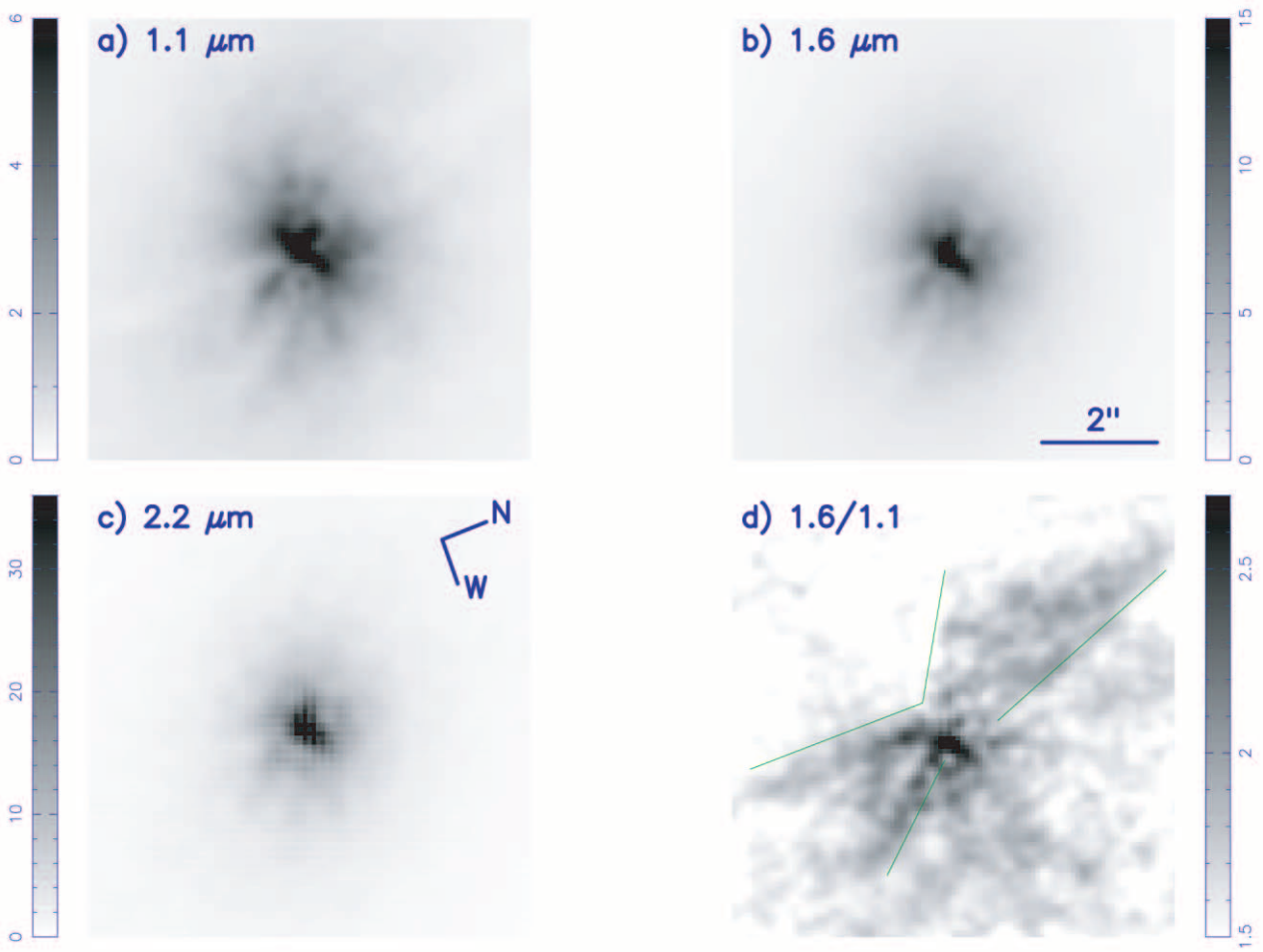

FIG. 1.—Deconvolved/Gaussian-smoothed images of nuclear regions of NGC 4418 at (*a*) 1.1 μm, (*b*) 1.6 μm, (*c*) 2.2 μm. The resolution of each image is 0.″14, and the associated scale bars are in units of microjanskys per pixel. Note the morphological similarities of the three images. (*d*) An $m_{1.1\mu m}-m_{1.6\mu m}$ image of the nuclear region of NGC 4418. The green lines outline the edges of the structure of the dark lanes visible in Figs. 1*a*–1*c* and Fig. 2, and the scale bar represents the ratio of the 1.6 and 1.1 μm flux densities provided in (*a*) and (*b*).

The main objective of the observational program was focused on obtaining mid-infrared photometry of a large number of sources. Hence only limited observations were made to constrain the size of NGC 4418. The observations of NGC 4418 were immediately followed by observations of Mrk 231 and HR 5340, both of which are assumed to be pointlike, i.e., the objects are assumed to be PSFs. These observations took nearly an hour. At 24.5 μm the PSFs throughout the night equaled the diffraction limit of the telescope; i.e., 0.″62 FWHM. At the shorter wavelengths the size of the PSF image was set by diffraction and the pixel sampling about half of the time throughout the night; at other times atmospheric seeing affected the image size. The variation in the measured size of the PSF calibration star is the largest uncertainty in the limit of the source size.

3. PHOTOMETRY

3.1. *Near-Infrared*

Carico et al. (1988) measured *J*, *H*, and *K* magnitudes of NGC 4418 of 12.97, 12.20, and 11.85, respectively, in a 5″ diameter beam. The corresponding $J-H$ and $H-K$ colors are 0.77 and 0.35, respectively. For comparison, magnitudes for the three NICMOS images were calculated using a 5″ beam and are measured to be $m_{1.1\mu m} = 13.22$ mag, $m_{1.6\mu m} = 12.21$ mag, and $m_{2.2\mu m} = 11.77$ mag (see also Table 2); the latter two measurements are within 0.1 mag of the *H* and *K* measurements by Carico et al. (1988). Interpolating the 1.25 μm magnitude from the 1.1 and 1.6 μm magnitudes, $m_{1.25\mu m}$ is determined to be 12.92 mag, which is also within 0.1 mag of the Carico et al. *J*-band measurement. Thus, $m_{1.1-1.6\mu m} = 1.00$ mag, $m_{1.25-1.6\mu m} = 0.71$ mag, and $m_{1.6-2.2\mu m} = 0.44$ mag. Subtracting the underlying galaxy from the nuclear component (within 1.″1, which is large enough to enclose the first Airy ring of a 2.2 μm NICMOS

TABLE 2
HST NICMOS PHOTOMETRY[a]

Wavelength (μm)	Nuclear[b] (mag)	1.″1 (mag)	5″ (mag)
1.1	16.04	14.98	13.22
1.6	14.78	13.85	12.21
2.2	14.05	13.26	11.77

[a] These measurements have also appeared in Scoville et al. 2000.

[b] Measured in a 1.″1 diameter beam with the underlying galaxy subtracted.

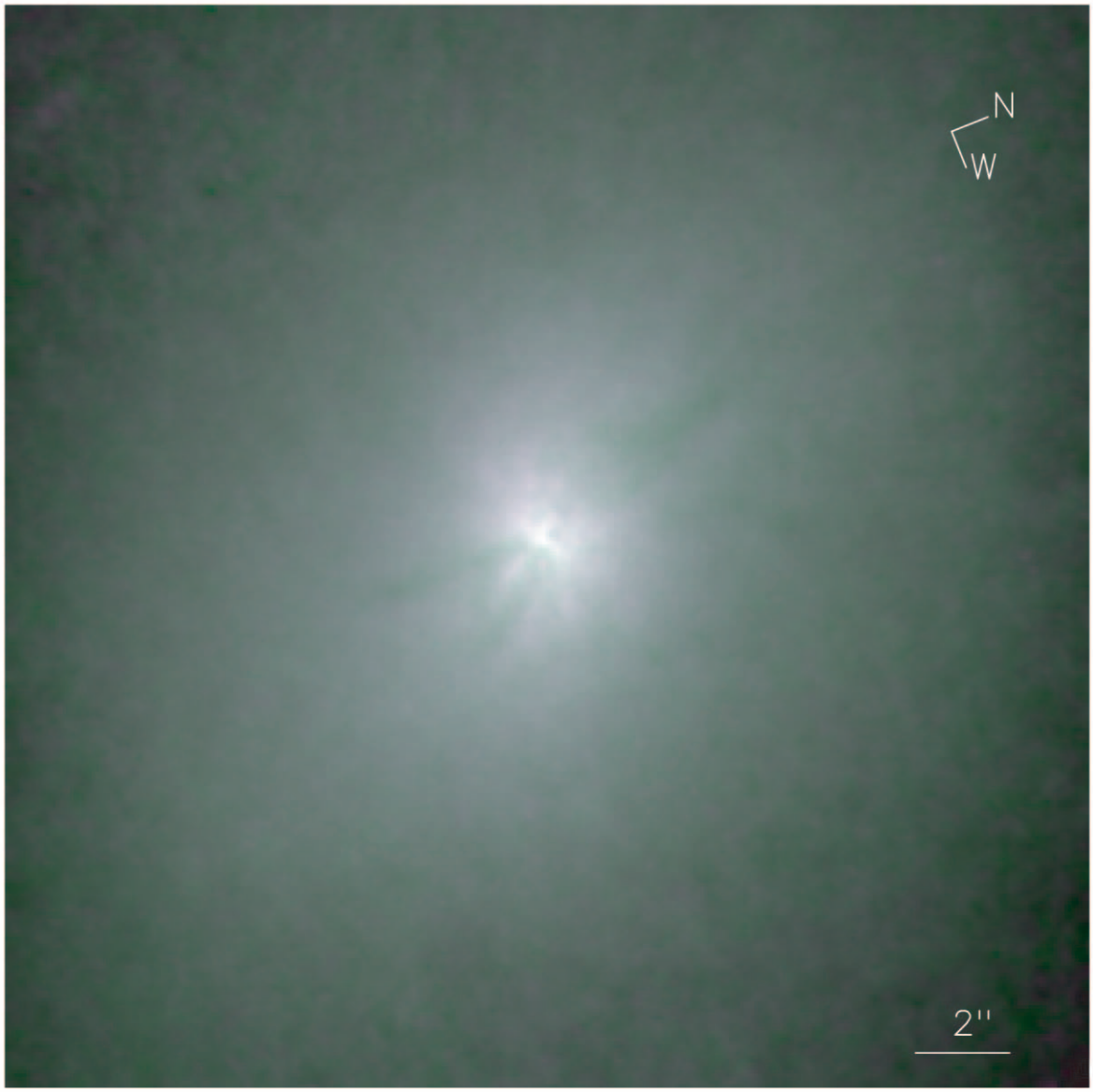

FIG. 2.—Composite of three infrared maps of NGC 4418 shown in false colors. The 1.1, 1.6, and 2.2 μm images are shown as blue, green, and red, respectively. The field of view is $\sim 11''.4 \times 11''.4$. The logarithm of each image was taken before combining the three wavelengths to compress the dynamic range.

PSF), yields $m_{1.1-1.6\mu m} = 1.26$ mag, $m_{1.25-1.6\mu m} = 0.88$ mag, and $m_{1.6-2.2\mu m} = 0.73$ mag.

3.2. *Mid-Infrared*

The mid-infrared photometric data are summarized in Table 1. The photometry was calibrated based on observations of the bright star HR 1457 ($=\alpha$ Tau) whose magnitudes, in turn, were based on *IRAS* photometry and intercomparisons with other bright stars over several nights. Only the statistical uncertainty is given in Table 1. The uncertainties in the photometry, based on the internal consistency of the observations, are estimated to be 5% at $\lambda \leq 17.9$ μm and 10% at 24.5 μm. The flux density corresponding to 0.0 mag (Vega-based) was taken to follow the prescription given in the Explanatory Supplement to the *IRAS* Catalogs and Atlases (Beichman et al 1989).

4. GENERAL CHARACTERISTICS OF THE NUCLEUS

4.1. *Near-Infrared*

Figures 1*a*–1*c* show gray-scale images of the nuclear region at 1.1, 1.6, and 2.2 μm. The inner 300 pc of NGC 4418 has a spider-like morphology. The highest surface brightness emission emanates from a central linear structure $\sim$100–200 pc across at a position angle of $\sim 110^{o}$. Fainter emission extends radially outward from the linear structure, with the highest surface brightness extension oriented perpendicular to the linear structure. The resultant T-like appearance of the higher surface brightness nuclear features is most apparent at 1.1 μm.

Figure 3 shows plots of the intensity profiles along the major axis of the linear structure. The intensity profile shows marked asymmetries, which may be due to extinction by foreground dust. The inner $\sim$3–4 pixels of each image are within a resolution element of the images—outside of

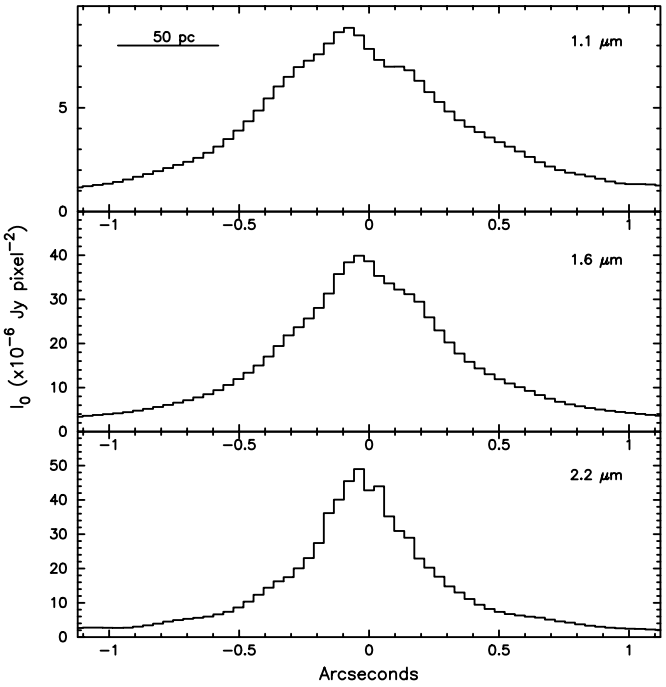

FIG. 3.—Intensity-profile plots of the nuclear structure. The profiles, which have a width of 0.″0386, have been extracted from the deconvolved/Gaussian-smoothed images.

this range, the intensity profiles initially decrease in a nearly Gaussian manner with radius, then exponentially. The width of the nucleus also decreases with wavelength; the full width at half the maximum intensity is 0.″80 (105 pc) at 1.1 μm and 0.″38 (50 pc) at 2.2 μm. Beyond a full width of 1.″82 (237 pc), the slopes of the profiles are shallow, and the intensity is most likely dominated by emission from the underlying galaxy.

In addition to the radial emission structures, two dark lanes extend radially southwest from the nucleus (see Fig. 2). A more diffuse dark lane extends in the northern direction.

4.2. *Mid-Infrared*

By a comparison with the sizes measured on HR 5340 and Mrk 231, NGC 4418 is unresolved at most mid-infrared wavelengths with these data. The upper limit depends on the wavelength, but subtracting the size of HR 5340 or Mrk 231 from NGC 4418 in quadrature yields a size of approximately 0.″23 (30 pc) diameter at 8 μm, and there is perhaps some evidence that it is marginally extended by around 0.″31 (40 pc) diameter in the silicate absorption feature near 10 μm. At 24.5 μm, the upper limit on the size is 0.″61 (80 pc).

5. DISCUSSION

These new near- and mid-infrared data provide a significant improvement in resolution relative to previously published data at these wavelengths; near-infrared images of NGC 4418 obtained by Zenner & Lenzen (1993) have a resolution between 0.″5 and 1.″3, and previously published 7–15 μm (Dale et al. 2000) and 12–25 μm (Wynn-Williams & Becklin 1993) data have resolutions of $\sim$8″ and 3″, respectively.

The near-infrared images of NGC 4418 are both striking and bemusing. In contrast to other luminous infrared galaxies imaged by NICMOS as part of the NICMOS GTO program (Scoville et al. 2000), the nucleus of NGC 4418 shows no direct evidence of star clusters. Nor is there evidence of an unresolved AGN as has been observed for warm luminous infrared galaxies such as NGC 7469 (e.g., Scoville et al. 2000). Instead, it consists of a resolved, central high surface brightness structure with light and dark features extending radially outward.

As discussed earlier, NGC 4418 has mid-infrared colors consistent with infrared galaxies observed to have Seyfert-like emission line spectra. However, unlike warm galaxies such as NGC 7469, the near-infrared colors of nucleus are not consistent with reddened AGN light (see Fig. 5 of Scoville et al. 2000). If the near-infrared emission is stellar in origin, then the age of the nuclear stellar population can be constrained by comparing its NICMOS colors with stellar population synthesis models in which the stellar light has been matched with the bandpasses of the NICMOS filters. Models have been derived for a 3–300 Myr Bruzual & Charlot (1993; 1995, private communication) instantaneous-starburst population having (1) a Salpeter initial mass function, (2) a mass range 0.1–125 $M_\odot$, (3) and solar metallicity. A comparison between these models and the nuclear colors of NGC 4418 shows the nuclear colors to be redder than the models. The application of the Rieke & Lebofsky (1985) extinction law show the nuclear colors to be consistent with a 10–300 Myr starburst suffering 2 (screen model) to 5 (dust mixed with stars model) magnitudes of visual extinction (see also Scoville et al. 2000). Near-infrared spectroscopy of NGC 4418 (Ridgway et al. 1994) shows a 2.3 μm CO absorption feature (in a 2.″7 diameter beam centered on the nucleus); the relative depth of the CO absorption feature and the slope of the continuum emission are consistent with a late-type supergiant or metal-rich giant population. If the near-infrared light from the nuclear feature is supergiant starlight with a few magnitudes of visual extinction, this would indicate that the supergiants responsible for the 2.3 μm absorption feature are in front of the bulk of the silicate grains responsible for the absorption feature of NGC 4418 at 9.7 μm (Roche et al. 1986; Spoon et al. 2001).

5.1. *Near- to Far-Infrared Spectral Energy Distribution*

Figure 4 is a spectral energy distribution (SED) of NGC 4418 using the photometry derived from the NICMOS and MIRLIN observations, combined with photometry from other sources (Carico et al. 1990; IRAS FSC 1990; Dale et al. 2000); the beam sizes are listed in the figure legend. For comparison, the ISO-PHT-S data from Spoon et al. (2001) are also plotted. Three key features of this SED are (1) a near-infrared thermal component which is likely due to the late-type supergiant population, (2) the shape of the MIRLIN SED at mid-infrared wavelengths which clearly shows the presence of the silicate absorption feature in NGC 4418 observed by Roche et al. (1986) and Spoon et al. (2001), and (3) the size of the 12 and 25 μm flux densities measured by *IRAS*, which are recovered by the unresolved MIRLIN emission at those wavelengths. From the latter two features, it can be concluded that the energy source(s) heating the silicate grains are confined to an area no more than 80 pc ($\sim$0.″6) across. Further, the highest-resolution radio map of NGC 4418 obtained to date shows the radio emission to be

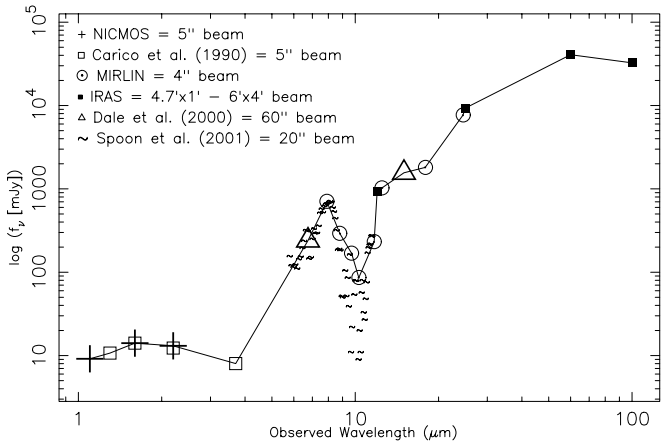

FIG. 4.—Spectral energy distribution of NGC 4418 based on broadband measurements. The solid line is a fit to the broadband data. Note the agreement between the broadband data and the ISO-PHT-S data.

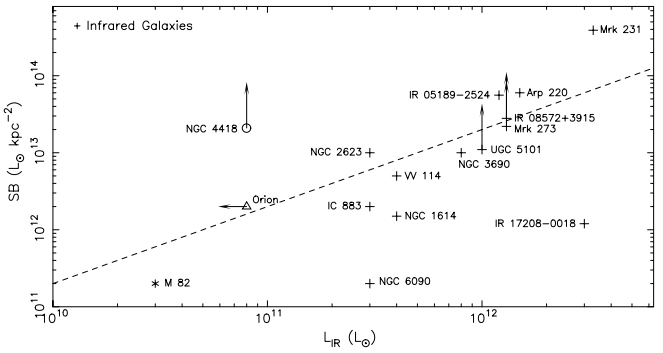

FIG. 5.—Plot of the infrared surface brightness vs. infrared luminosity for NGC 4418 and a sample of objects discussed in Soifer et al. (2000, 2001). The dashed curve is an example of an isosurface area curve; all such curves on Fig. 5 are parallel to the dashed curve.

less than 0.″47 in extent (Eales et al. 1990), providing further proof of the importance of the inner 80 pc to the total energy output of the galaxy.

5.2. *Far-Infrared Size Constraint and Surface Brightness*

Even given the overwhelming evidence at mid-infrared and radio wavelengths that the energy sources in NGC 4418 are confined in a nuclear region no more that 80 pc across, a direct measurement at the wavelength where most of the energy of NGC 4418 is emanating from—the far-infrared—is ideally desired. High-resolution imaging of the galaxy at these wavelengths is not presently possible, however, additional support for a compact far-infrared emission region can be provided via two approximations.

For the first approximation, the assumption is made that the nuclear dust that is reradiating light from the imbedded nuclear source(s) in NGC 4418 is distributed in an optically thick sphere of diameter D and outer blackbody temperature, $T_{\rm dust}$. The dust temperature is calculated from the 60 and 100 μm flux densities $f_{60\mu{\rm m}}$ and $f_{100\mu{\rm m}}$ via the equation

$$T_{\rm dust} = -(1+z)\left[\frac{82}{\ln(0.3 f_{60\mu{\rm m}}/f_{100\mu{\rm m}})} - 0.5\right] \qquad (1)$$

(e.g., see Solomon et al. 1997). For $f_{60\mu{\rm m}} \sim 40.68$ Jy and $f_{100\mu{\rm m}} \sim 32.80$ Jy, $T_{\rm dust} \sim 85$ K. The blackbody diameter is thus calculated via the equation

$$D = 2\left(\frac{L_{\rm IR}}{4\pi\sigma T_{\rm dust}^4}\right)^{0.5}, \qquad (2)$$

where σ is the Stefan-Boltzmann constant, which yields a diameter of 0.″54 (70 pc). This is equivalent to the upper size limit of the 25 μm and radio emission of NGC 4418, as well as the FWHM of its 2.2 μm emission. Note that a source with a brightness temperature of 85K and a flux density of 9.32 Jy at 25 μm has a diameter of 0.″41 (53 pc), which is also consistent with the measured upper limit of the 25 μm emission.

If the dust emitting the far-infrared emission is associated with the star-forming molecular gas in NGC 4418, the distribution of this gas in the nucleus of NGC 4418 can be used as an independent second approximation to the extent of the far-infrared emission. No interferometric CO(1→0) data presently exist of NGC 4418, however single-dish measurements have been made which provide a CO luminosity, $L'_{\rm CO}$, and a velocity dispersion. Using these data, the assumption is made that the brightness temperature of the CO(1→0) emission is equal to the dust temperature and that the gas has a unity filling factor. Thus, the CO diameter, $D_{\rm CO}$, is derived via

$$D_{\rm CO} = 2\sqrt{\frac{L'_{\rm CO}}{\pi T_{\rm bb}\Delta v_{\rm FWHM}}}, \qquad (3)$$

where $\Delta v_{\rm FWHM}$ is the full width at half the maximum intensity velocity width (= 120 km s^{-1}; Sanders et al. 1991). The CO diameter is calculated to be 1.″5 (200 pc).

If the size of 70 pc is adopted for the mid- to far-infrared emission region, then the surface brightness of NGC 4418 is calculated to be $4L_{\rm IR}/\pi{\rm D}^2 \sim 2.1 \times 10^{13}\ L_\odot$ kpc^2. Figure 5 is a plot of infrared surface brightness versus infrared luminosity for a sample of galaxies imaged at mid-infrared wavelengths by Soifer et al. (2000; 2001), as well as the Orion star-forming complex and M82 (see also Soifer et al. 2001). The surface brightness of NGC 4418 is extreme, being comparable to that of the warm ultraluminous infrared galaxies (e.g., IRAS 05189−2524, IRAS 08572+3915, and Mrk 231) and cool ultraluminous infrared galaxies ($f_{25\mu{\rm m}}/f_{60\mu{\rm m}} < 0.2$; which may be powered primarily by a starburst, AGN, or both) such as Arp 220, UGC 5101, and Mrk 273, a factor of 100 larger than that of M82, and a factor of 10 larger than that of the star-forming complex in Orion.[11] In comparison with starburst galaxies with infrared luminosities moderately higher than NGC 4418 (i.e., NGC 1614, NGC 2623, IC 883, NGC 6090, Mrk 331; Soifer et al. 2001), NGC 4418 has an infrared surface brightness a factor of 2–100 higher. From the limited number of objects plotted in Figure 5, there is no clear indication that infrared surface brightness alone can be used as a diagnostic between AGN and starburst energy sources.

[11] Note that, with the exception of Arp 220, UGC 5101, and IR 17208−0018, all of the ultraluminous infrared galaxies plotted in Fig. 5 show strong evidence of being powered by an AGN (i.e., based on the presence of broad recombination emission lines, warm mid-infrared colors, and/or AGN-like X-ray emission).

5.3. *Dark Lanes*

As previously mentioned, dark lanes are observed to be associated with the central high surface brightness near-infrared peak of NGC 4418. Figure 1*d* shows an $m_{1.1\mu m}-m_{1.6\mu m}$ image of NGC 4418; in this image, the dark lanes appear as cones extending away from the nucleus.

There are two likely explanations for the nature of the dark lanes in the nucleus of NGC 4418. The first possibility is that the features are dust lanes. Such radial dust lanes are observed in the nucleus of spiral galaxy M51, albeit on a smaller scale (50 pc: Grillmair 1997 and references therein). The presence of such dust lanes, if they lie in the foreground of the nuclear infrared disk, may explain the asymmetries observed in Figure 3, however, it is difficult to understand why such radial dust lanes have not been destroyed by rotation.

The second possible explanation for the dark lanes is that they are shadows cast from a partially obscured AGN. Such a possibility would require that the AGN be visible along lines of sight that lie within the plane of the sky, but also require that certain lines of sight toward the AGN in the plane of the sky are blocked, perhaps by the presence of molecular clouds.

These two possibilities can be tested. First, if AGN light is visible along lines of sights within the plane of the sky, then near-infrared, low surface brightness light surrounding the inner nucleus should be polarized. Second, if the dark lanes are nuclear dust lanes, CO(1→0) observations of NGC 4418 should reveal evidence of molecular gas coincident with the lanes. Such CO observations would be useful in their own right as a confirmation of the high extinction to the nucleus calculated via the silicate absorption feature.

5.4. *A Portrait of NGC 4418*

Given the new data presented in this paper and compiled from the literature, NGC 4418 appears to be a galaxy with nuclear power source(s) which has (have) been triggered via interactions with a companion galaxy 24 kpc away. The galaxy NGC 4418 has the following near- to mid-infrared properties:

1. a compact, near-infrared nucleus consisting of a 100–200 pc high surface brightness linear feature surrounded by radial extensions and near-infrared colors consistent with moderately extinguished supergiant stellar light;
2. no nuclear star clusters at near-infrared wavelengths, which are commonly seen in starburst infrared galaxies, and no bright pointlike nucleus commonly seen in AGNs;
3. an infrared surface brightness comparable to warm ultraluminous infrared galaxies and cool ultraluminous infrared galaxies, such as Arp 220 and UGC 5101;
4. emission of most of its mid- to far-infrared light from a region $\lesssim 80$ pc across;
5. a deep silicate absorption feature, which translates into greater than 50 mag of visual extinction to the central energy source(s) (see also Roche et al. 1986; Dudley & Wynn-Williams 1997; Spoon et al. 2001);
6. no evidence of strong PAH features, which are common to mildly extinguished starburst galaxies such as M82 (Genzel et al. 1998; Spoon et al. 2001); and
7. warm infrared colors ($f_{25\mu m}/f_{60\mu m} = 0.23$) consistent with those observed for infrared galaxies with Seyfert-like emission-line spectra.

The basic picture of NGC 4418 is one in which a stellar core/disk approximately 150 pc in extent surrounds an imbedded AGN or a compact starburst. So deeply buried is the central engine(s) that even probing the galaxy at near-infrared wavelengths, where extinction is 5–10 mag, rather than 50–100 mag at optical wavelengths, provides little information about the primary energy source in NGC 4418. Observations at longer wavelengths, using instruments such as MIRLIN, *Satellite Infrared Telescope Facility* (*SIRTF*), and the Stratospheric Observatory for Infrared Astronomy (SOFIA), will be required to determine the fundamental nature of this galaxy class.

We thank B. Stobie, J. Mazzarella, D. Dale, A. Sargent, and L. Armus for useful discussions and assistance, and the anonymous referee for a careful reading of the manuscript. A. S. E. also thanks H. Spoon for providing ISO-PHT-S data for inclusion in Figure 4. A. S. E. and N. Z. S. were supported by NASA grant NAG 5-3042. A. S. E. was also supported by NSF grant AST 02-06262. This research has made use of the NASA/IPAC Extragalactic Database, which is operated by the Jet Propulsion Laboratory, California Institute of Technology, under contract with NASA.

REFERENCES

Armus, L., Heckman, T. M., & Miley, G. K. 1989, ApJ, 347, 727
Beichmann, C. A., Neugebauer, G. H., Habing, H. J., Clegg, P. E., & Chester, T. J. 1989, *IRAS* Catalog and Atlases, Explanatory Supplement (2d ed.; Washington: GPO)
Bruzual, G. A., & Charlot, S. 1993, ApJ, 405, 538
Bushouse, H. 1997, in *HST* Calibration Workshop, ed. S. Casertano, R. Jedrzejewski, T. Keyes, & M. Stevens (Baltimore: STScI), 223
Carico, D. P., Sanders, D. B., Soifer, B. T., Elias, J. H., Matthews, K., & Neugebauer, G. 1988, AJ, 95, 356
Carico, D. P., Sanders, D. B., Soifer, B. T., Matthews, K., & Neugebauer, G. 1990, AJ, 100, 70
Dale, D. A., et al. 2000, AJ, 120, 583
Dudley, C. C., & Wynn-Williams, C. G. 1997, ApJ, 488, 720
Eales, S. A., Becklin, E. E., Hodapp, K. W., Simons, D. A., & Wynn-Williams, C. G. 1990, ApJ, 365, 478
Genzel, R. et al. 1998, ApJ, 498, 579
Grillmair, C. J., Faber, S. M., Lauer, T. R., Hester, J. J., Lynds, C. R., O'Neil, E. J., & Scowen, P. A. 1997, AJ, 113, 225
Hook, R. N., & Fruchter, A. S. 1997, in ASP Conf. Ser. 125, Astronomical Data Analysis, Software, and Systems VI, ed. G. Hunt & E. Payne (San Francisco: ASP), 147
Ressler, M. E., Werner, M. W., Van Cleve, J., & Choa, H. 1994, Exp. Astron., 3, 277
Ridgway, S. E., Wynn-Williams, C. G., & Becklin, E. E. 1994, ApJ, 428, 609
Rieke, G. H., & Lebofsky, M. J. 1985, ApJ, 288, 618
Roche, P. F., Aitken, D. K., Smith, C. H., & James, S. D. 1986, MNRAS, 218, P19
Sanders, D. B., & Mirabel, I. F. 1996, ARA&A, 34, 749
Sanders, D. B., Scoville, N. Z., & Soifer, B. T. 1991, ApJ, 370, 158
Scoville, N. Z., et al. 2000, AJ, 119, 991
Smith, C. H., Aiken, D. K., & Roche, P. F. 1989, MNRAS, 241, 425
Soifer, B. T., et al. 2000, AJ, 119, 509
———. 2001, AJ, 122, 1213
Solomon, P. M., Downes, D., Radford, S. J. E., & Barrett, J. W. 1997, ApJ, 478, 144
Spoon, H. W. W., Keane, J. V., Tielens, A. G. G. M., Lutz, D., & Moorwood, A. F. M. 2001, A&A, 365, L353
Thompson, R. I., Rieke, M., Schneider, G., Hines, D. C., & Corbin, M. R. 1998, ApJ, 492, L95
Wynn-Williams, C. G., & Becklin, E. E. 1993, ApJ, 412, 535
Zenner, S., & Lenzen, R. 1993, A&AS, 101, 363